Silicon Clusters of Intermediate Size: Energetics, Dynamics, and Thermal Effects

Lubos Mitas,[1] Jeffrey C. Grossman,[2] Ivan Stich,[3,4] and Jaroslav Tobik[3]

[1]*National Center for Supercomputing Applications, University of Illinois at Urbana-Champaign, Urbana, Illinois 61801*
[2]*Department of Physics, University of California at Berkeley and Materials Sciences Division, Lawrence Berkeley National Laboratory, Berkeley, California 94720*
[3]*Slovak Technical University (FEI), Department of Physics, Ilkovičova 3, 812 19 Bratislava, Slovakia*
[4]*Joint Research Center for Atom Technology & Angstrom Technology Partnership, 1-1-4 Higashi, Tsukuba, Ibaraki 305, Japan*

(Received 14 October 1999)

A combination of the best available theoretical techniques for energetics, dynamics, and thermodynamics is employed in an extensive study of Si_n ($n = 20, 25$) clusters. For $T = 0$ we solve the electronic structure by the density functional and the highly accurate quantum Monte Carlo approaches. Finite temperature and dynamical effects are investigated by the *ab initio* molecular dynamics method. This combination of methods enables us to find several new low-energy isomers and to explain the differences in properties, behavior, and stability of elongated versus compact types of structures and to elucidate the origin of the existing discrepancies between theory and experiments.

PACS numbers: 61.46.+w, 36.40.–c, 71.15.Nc, 71.24.+q

The study of atomic clusters has become one of the most active areas of research over the last decade. The main reasons for such an intense interest can be stated as follows: (i) fundamental importance of understanding properties of materials with increasing size, especially the transition molecule → cluster → bulk; (ii) experimental techniques for production and analysis of clusters has improved dramatically, providing new data about their electronic, chemical, and structural properties; (iii) crucial role of clusters in a number of industrial applications such as catalysis or in a development of new semiconducting/magnetic devices; and (iv) use of clusters as building blocks ("superatoms") to synthesize new solid or surface materials. In this Letter we carry out a thorough study of Si_n clusters for $n = 20$ and 25 which bracket the range of sizes with known discrepancies between theory and experiments [1–3] and exemplify a variety of isomers found in this size range which have been the subject of several previous theoretical studies [2,4–13]. Our focus is the prolate → oblate structural transition [1], in particular, the corresponding structures and energetic ordering of low-lying isomers and the impact of dynamical and temperature effects. To resolve these issues we use a combination of the best theoretical tools currently available, namely, the density functional theory (DFT) and quantum Monte Carlo (QMC) electronic structure methods and the *ab initio* molecular dynamics (MD).

The agreement between theory and experiment for Si clusters with less than 20 atoms appears to be very good [2]; however, starting from Si_{20} discrepancies between the energy ordering of the known isomers and experimental spectra become visible. In particular, the experiments indicate an onset of prolate → oblate structural transition which poses an interesting challenge for theory and which is still unsolved despite a number of papers on this subject in the past. The elusive character of our understanding of this phenomenon can be illustrated, for example, by evolving suggestions for the most stable Si_{20} structures [2,5,7,12,13], with an accumulated gain in the total energy by almost 5 eV. Moreover, while the experimental mobility spectra at this size clearly favored the elongated structures, the recent theoretical predictions of Ho *et al.* [2] favored the spherical-like geometry. In order to explain the source of this discrepancy, we investigate the following possibilities: (i) the previous electronic structure calculations are not accurate enough; (ii) the actual atomic structures in question are not known; (iii) dynamical and finite temperature effects are not accounted for; (iv) the barriers for spontaneous creation of elongated versus spherical structures are significant; and (v) the structure and/or energetics of the charged clusters studied in the experiments [1] could be different from the neutral ones. The combination of DFT and QMC methods enable us to investigate the importance of (i), (v), and to some extent (iv), and equipped with this knowledge the finite-temperature *ab initio* MD method allows us to investigate the importance of (ii) and (iii).

For $T = 0$ DFT calculations, we employ the commonly used approaches of the local density approximation (LDA) and generalized gradient approximations (GGAs) with the BPW91, BLYP, B3PW91, and B3LYP functionals [15–17]. It has been shown that these methods may not be accurate enough for predicting energy differences of clusters [6] and therefore we check some of the results by QMC. QMC has the advantage that many-body correlation effects are described directly through an explicit correlation of the trial wave function and through a stochastic solution of Schrödinger equation. The trial wave function is a product of Slater determinants with spin-up and spin-down orbitals and a correlation factor

$$\Psi_T = Det^{\uparrow}\{\varphi_\alpha\} Det^{\downarrow}\{\varphi_\beta\} \exp\left[\sum_{I,i<j} u(r_{iI}, r_{jI}, r_{ij})\right]. \quad (1)$$

The correlation factor describes electron-electron and electron-electron-ion many-body effects through the explicit dependence on distances between electrons (r_{ij}) and between electrons and ions (r_{iI}, r_{jI}). To obtain the accuracy beyond the variational ansatz we solve the Schrödinger equation using the diffusion Monte Carlo method in the fixed-node approximation [6,18,19]. The fixed-node solution Φ is found by iterating the equation

$$f(\mathbf{R}, t + \tau) = \int G(\mathbf{R}, \mathbf{R}', \tau) f(\mathbf{R}', t)\, d\mathbf{R}', \qquad (2)$$

where

$$G(\mathbf{R}, \mathbf{R}', \tau) = \Psi_T(\mathbf{R}) \langle \mathbf{R}| \exp(-\tau H) |\mathbf{R}'\rangle / \Psi_T(\mathbf{R}'), \quad (3)$$

$f(\mathbf{R}, t) = \Psi_T(\mathbf{R})\Phi(\mathbf{R}, t)$, t is the imaginary time, and $\mathbf{R}$ denotes the coordinates of electrons. H is the usual Hamiltonian of interacting electrons and ions with core electrons eliminated by nonlocal pseudopotentials so that in QMC we explicitly treat only the valence electrons. The impact of pseudopotential on the accuracy of Si QMC results has been tested in our previous calculations [6,13,19] and was found to be negligible, i.e., below our statistical error bars. Finally, typical errors for energy differences from the fixed-node approximation is 1%–2% [18] which, in our case, is below the obtained error bars.

To understand the $T > 0$ behavior we use the *ab initio* MD [20] method with the BPW91 functional to describe the electronic degrees of freedom. Simulations have been done close to the experimental conditions at $T = 300$ K and then at high temperatures $T \sim 1000$–3000 K for assessment of stability of different structures. All finite temperature calculations have been done in the canonical ensemble using plane-wave [21] pseudopotential techniques [20,22]. We found that a MD observation time of $\sim$2 ps was sufficient for a structural sampling of the potential energy surface as well as for characterizing the cluster stability. We also checked that the 6-311G* [17] Gaussian basis set used for the DFT methods, equivalent of 6-311G* used for the Hartree-Fock (HF) pseudopotential method and the mentioned cutoff [21] in the MD/DFT pseudopotential approach were sufficient for providing the correct energy differences within 0.1 eV.

We consider a set of five possible low-energy structures of the Si_{20} cluster shown in Fig. 1. The elongated *A* and the spherical-like *B* structure were suggested by Ho *et al.* [2] using a genetic optimization algorithm. *A* is composed of two very stable Si_{10} units while *B* is a strongly distorted dodecahedron with one of the pentagons broken (one of the broken pentagon atoms saturates the dangling bonds in the dodecahedron interior while the four remaining atoms are relaxed into a new bonding pattern). Structure *C* was suggested by Song *et al.* [7] and comes from an *ab initio* DFT relaxation of the dodecahedron which converged to a "squished" dodecahedron structure with extensive rebonding and restructuring. Structure *D* was constructed by us

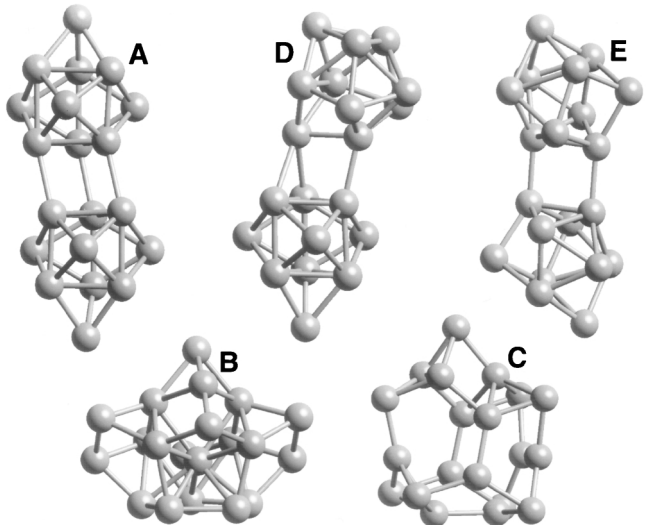

FIG. 1. Structures of five studied low-energy isomers (see text) of the Si_{20} cluster.

by matching the lobes of the highest occupied molecular orbitals of the open-shell Si_9 and Si_{11} clusters with a subsequent optimization. Finally, the structure *E* was obtained by taking snapshots from our $T = 300$ K MD run (see below) with a subsequent relaxation to $T = 0$. Evidently, *A*, *D*, and *E* belong to the same "$Si_{10} + Si_{10}$" class of elongated structures [2,3].

In order to clarify the accuracy of the different electronic structure methods we show in Table I our results for energy differences computed with HF, GGAs, and QMC methods. The table illustrates clearly several important trends. First, note that HF favors the structure *C* and disagrees therefore with the rest of the methods which is a clear indication that electron correlation effects are important. Second, most LDA/GGA approaches favor the compact *B* structure with structure *E* being close, and for functionals with the LYP correlation functional the *E* structure is actually below *B* although only by a small amount. The bias of the DFT methods towards more compact structures is well-known and can be rationalized by the DFT tendency to homogenize and increase the electron density of the system. It

TABLE I. Energy differences (eV) for five LDA optimized geometries (see Fig. 1), listed for each method relative to the total energy of structure *B*. All HF and DFT energies are computed using the 6-311G* basis set. For QMC values, the statistical errors are in parenthesis.

Si_{20}	*A*	*B*	*C*	*D*	*E*
HF	1.96	0.00	−0.58	1.84	−0.11
LDA	0.76	0.00	1.33	0.83	0.53
BPW91	0.45	0.00	0.92	0.58	0.26
B3PW91	0.87	0.00	0.83	0.85	0.32
BLYP	0.23	0.00	0.26	0.40	−0.20
B3LYP	0.70	0.00	0.29	0.71	−0.05
QMC	0.19(5)	0.00	0.60(5)	0.16(5)	−0.65(5)

is also useful to notice how strongly LDA favors structure B and how the GGA functionals decrease this difference; however, the correction is nonsystematic and does not enable one to predict the actual energy ordering of the structures. Third, the QMC method shows that the impact of electron correlation on the energy differences is important (0.5–1.0 eV). QMC also clearly shows that it is the structure E which is actually the lowest in energy, while structures A and D are within 0.2 eV from the structure B. In favor of the structure E speaks also its (vertical) ionization potential of 7.3 eV in BPW91 which agrees favorably with the experimental value 7.5(1) eV [2,3]. This can be compared, for example, with structure A having the corresponding ionization potential of 6.9 eV. Our results for ionized clusters which are actually being observed in experiments confirmed our results from the neutral cases and show the ionization potential for structure E to be the largest and in agreement with the experiment.

One of the surprising features we have observed in the zero temperature results is the flatness of the potential energy surface around structural minima. We have found that the isomers showed structural differences when optimized with different functionals; nevertheless, the impact on energy differences has been minimal. For example, the BLYP and LDA optimized structures A differ by as much as two bonds, while energetically the two structures are very close. We confirmed this also by QMC in which the energies of BLYP and LDA optimized structures A came out within our QMC statistical error of 0.05 eV. Thus, we have concluded that the different sets of optimized geometries were essentially equivalent and that the relative energies of isomers in Table I were dominated by the choice of methods and functionals.

The dynamical simulations further elucidated the structural behavior and stability of the competing structures. The low temperature runs ($T = 300$ K) revealed a dynamical pattern of bond stretching and bond breaking of one or two bonds with subsequent rebonding in rather short time intervals ($\sim$0.1 ps). Nevertheless, during the entire simulations both A and B structures remained in essentially the same structural pattern (i.e., in elongated and spherical-like configuration, respectively). We also took several snapshots from the $T = 300$ K MD trajectories of structures A and B and relaxed them to the $T = 0$ ground state. In this way we found the energetically most stable structure E. On the other hand, the snapshots which initiated from structure B remained all within $\sim$0.01 eV of the initial structure upon subsequent $T = 0$ optimization, indicating that, at this temperature, structure B is significantly more "rigid" than A.

In addition, we checked the stability of the structures by increasing the temperature to 1000 and 1500 K. At the higher temperature, structure A broke into two strongly deformed Si_{10} units in about 0.5 ps. Breaking of structure A into two Si_{10} subunits also indirectly points out the possible mechanism for formation of the elongated structures. It is relatively easy to create structure A from two Si_{10} units which are abundant. The temperature of dissociation suggests that the actual barrier is rather low, most likely below 1 eV, although one has to keep in mind the limited accuracy of the PW91 GGA functional. On the other hand, it is much more difficult to find a corresponding mechanism for structure B as the decomposition of B into stable units is less obvious and most probably involves a sequence of additions of units smaller than Si_{10}, i.e., additions of Si_m ($m \approx 2$–5) which are energetically much less stable and less favorable. Therefore, spontaneous creation of structure B is likely to proceed in a number of steps with barriers corresponding to a few bond formations per step which contrasts with structure A where there is only a single barrier to overcome. The dynamical simulation confirmed this picture. Heating structure B to 1500 K did not lead to structural breakdown on our MD observation time scale. Only after heating B to 3000 K did we observe a rapid breakdown into a number of volatile and reactive fragments. This suggests that the decomposition is a concerted process with significantly higher energy barrier. From our dynamical $T > 0$ simulations we predict that structure B is rather stable, but its formation would require a number of intermediate structures so that the overall probability of appearing in the spectrum is quite low. This contrasts with the abundance of Si_{10} which can readily fuse into low energy isomers such as E.

Using a combination of MD and $T = 0$ relaxation we were able to construct a number of new elongated and spherical-like structures also for Si_{25}. The lowest-energy isomers from both families (elongated, spherical) we have found are shown in Fig. 2. The energy differences are very small as the compact structure is lower by only 0.15 eV in PW91 and 0.63 eV in LDA thus, as suggested by experiment [1], corroborating the existence of both structural branches in this range of sizes.

It is interesting to note that the Si_{25} elongated cluster has structural features of both Si_{10} type units and also a sixfold puckered ring, a typical building block in previous studies [5,6,12,13]. On the other hand, the $N = 25$ compact structure shows an intriguing structural feature of "internal" atoms which are encapsulated in the distorted cage-like configurations formed of the "surface" atoms. This is similar to the feature observed in larger spherical clusters with 33 to 45 atoms in which a small cage appeared encapsulated into a larger one [14]. In fact, cluster B of Si_{20} can be considered a precursor of this structural type with one of the atoms being at the center of a partially opened distorted dodecahedron. The internal atoms fulfill two important roles. First, they saturate the dangling bonds [14] of the surface atoms which would otherwise be mostly threefold coordinated (the predominant coordination for silicon in clusters is 4-5). Second, studies of structural relaxation and dynamics suggest that the internal atoms act as "catalytic" centers: their high coordination and multiple weak bonds enable structures to relax through

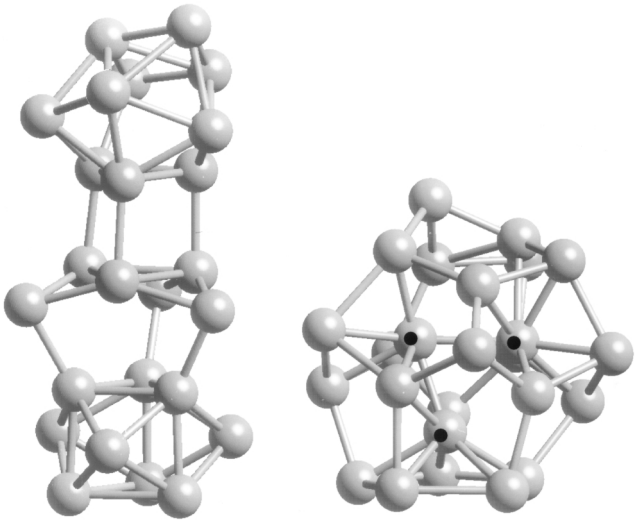

FIG. 2. Structures of two low-energy isomers from the elongated and spherical families of Si_{25} clusters. The "internal" atoms discussed in the text are denoted by black circles.

a sequence of rebonding and restructuring steps. This also suggests a mechanism for the system to surpass the large energy barriers in the formation process of larger compact structures. We conjecture that it is the interplay of both structural and dynamical mechanisms which is responsible for the transition from prolate to oblate observed in experiments.

In conclusion, our findings can be summarized as follows: (a) electron correlation has an important effect on the overall stability of silicon cluster isomers and high accuracy such as quantum Monte Carlo methods are necessary to predict the true energetic ordering; (b) the *ab initio* dynamical ($T = 300$ K) simulations show that the energy surfaces of the silicon clusters are very flat with one or two bond breaking and subsequent rebonding appearing on a time scale of $\sim$0.1 ps, without a significant change in the overall structure; (c) the structural transition from elongated to compact structures is related to the onset of formation of structures composed of irregular cages with a small number of encapsulated atoms which have both structural and dynamical roles in the formation process. Our results demonstrate that combination of energetic, dynamical, and thermal studies using the state-of-the-art methods provides a unique and revealing picture of the Si_n cluster systems. The wealth of structural and dynamical information obtained in the present work enabled us to understand the distinct properties of elongated versus compact types of structures, to generate the lowest energy isomers known so far, and to suggest a mechanism which drives the experimentally observed transition between these two types of conformation in the range of $20 \leq n \leq 25$.

We acknowledge communications and discussions with A. A. Shvartsburg, M. F. Jarrold, and D. A. Drabold. This research has been supported by U.S. DOE, by JRCAT (Japan), and by the State of Illinois. Part of the work has been done at the Aspen Center for Theoretical Physics Workshop in 1998, and its support is gratefully acknowledged as well (L. M. and J. C. G.).

[1] M. F. Jarrold, J. Phys. Chem. **99**, 11 (1995).
[2] K. M. Ho, A. A. Shvartsburg, B. Pan, Z. Y. Lu, C. Z. Wang, J. G. Wacker, J. L. Fye, and M. F. Jarrold, Nature (London) **392**, 582 (1998).
[3] A. A. Shvartsburg, M. F. Jarrold, B. Liu, Z. Y. Lu, C. Z. Wang, and K. M. Ho, Phys. Rev. Lett. **81**, 4616 (1998).
[4] J. C. Phillips, J. Chem. Phys. **87**, 1712 (1987).
[5] E. Kaxiras and K. Jackson, Phys. Rev. Lett. **71**, 727 (1993).
[6] J. C. Grossman and L. Mitas, Phys. Rev. Lett. **74**, 1323 (1995).
[7] J. Song, S. E. Ulloa, and D. A. Drabold, Phys. Rev. B **53**, 8042 (1996).
[8] N. Binggeli and J. R. Chelikowsky, Phys. Rev. B **50**, 11 764 (1994).
[9] E. C. Honea, A. Ogura, C.A.Murray, K. Raghavachari, W. O. Sprenger, M. F. Jarrold, and W. L. Brown, Nature (London) **366**, 42 (1993).
[10] B. Liu, A. A. Shvartsburg, Z. Y. Lu, B. Pan, C. Z. Wang, K. M. Ho, and M. F. Jarrold, J. Chem. Phys. **109**, 9401 (1998).
[11] U. Röthlisberger, W. Andreoni, and P. Gianozzi, J. Chem. Phys. **96**, 1248 (1992).
[12] M. R. Pederson, K. Jackson, D. V. Porezag, Z. Hajnal, and T. Frauenheim, Phys. Rev. B **54**, 2863 (1996).
[13] J. C. Grossman and L. Mitas, Phys. Rev. B **52**, 16 735 (1995).
[14] U. Röthlisberger, W. Andreoni, and M. Parrinello, Phys. Rev. Lett. **72**, 665 (1994).
[15] P. Hohenberg and W. Kohn, Phys. Rev. **136**, B864 (1964); W. Kohn and L. J. Sham, Phys. Rev. **140**, A1133 (1965).
[16] J. P. Perdew, in *Electronic Structure of Solids '91*, edited by P. Ziesche and H. Eschrig (Akademie Verlag, Berlin, 1991), p. 11, and references therein; A. D. Becke, Phys. Rev. A **38**, 3098 (1988); J. Chem. Phys. **98**, 5648 (1993); **104**, 1040 (1996).
[17] M. J. Frisch *et al.*, GAUSSIAN 94 (Gaussian Inc., Pittsburgh, PA, 1995).
[18] L. Mitas, Comput. Phys. Commun. **96**, 107 (1996); D. M. Ceperley and L. Mitas, in *Advances in Chemical Physics*, edited by I. Prigogine and S. A. Rice (Wiley, New York, 1996), Vol. XCIII, p. 1, and references therein.
[19] L. Mitas, E. L. Shirley, and D. M. Ceperley, J. Chem. Phys. **95**, 3467 (1991).
[20] See, for instance, M. C. Payne, M. P. Teter, D. C. Allan, T. A. Arias, and J. D. Joannopoulos, Rev. Mod. Phys. **64**, 1045 (1992).
[21] We use a plane wave cutoff of 10 Ryd.
[22] L. J. Clarke, I. Stich, and M. C. Payne, Comput. Phys. Commun. **72**, 14 (1992).